Predicting strength development of RMSM using ultrasonic pulse velocity and artificial neural network

Nain Y. Sheen[a], Jeng L. Huang[b] and Hien D. Le[*]

Department of Civil Engineering, National Kaohsiung University of Applied Sciences,
415 Chien Kung, Kaohsiung 807, Taiwan, ROC

Abstract. Ready-mixed soil material, known as a kind of controlled low-strength material, is a new way of soil cement combination. It can be used as backfill materials. In this paper, artificial neural network and non-linear regression approach were applied to predict the compressive strength of ready-mixed soil material containing Portland cement, slag, sand, and soil in mixture. The data used for analyzing were obtained from our testing program. In the experiment, we carried out a mix design with three proportions of sand to soil (e.g., 6:4, 5:5, and 4:6). In addition, blast furnace slag partially replaced cement to improve workability, whereas the water-to-binder ratio was fixed. Testing was conducted on samples to estimate its engineering properties as per ASTM such as flowability, strength, and pulse velocity. Based on testing data, the empirical pulse velocity–strength correlation was established by regression method. Next, three topologies of neural network were developed to predict the strength, namely ANN-I, ANN-II, and ANN-III. The first two models are back-propagation feed-forward networks, and the other one is radial basis neural network. The results show that the compressive strength of ready-mixed soil material can be well-predicted from neural networks. Among all currently proposed neural network models, the ANN-I gives the best prediction because it is closest to the actual strength. Moreover, considering combination of pulse velocity and other factors, viz. curing time, and material contents in mixture, the proposed neural networks offer better evaluation than interpolated from pulse velocity only.

Keywords: ready-mixed soil material; ultrasonic pulse velocity; neural network; back-propagation; radial basis function

1. Introduction

Ready-mixed soil material (RMSM) is known as a kind of controlled low-strength material (CLSM) (ACI 229 2005) when a large amount of soil is used as fine constituent. RMSM is a new combination of soil and cement; and it has been successfully applied to numerous fields such as backfill wall or trench fill, void filling, and pavement bases (Green 1999, Wu 2005, Finney *et al.* 2008, Wu and Lin 2011). Similar to general CLSM, RMSM has some advantages, viz. easy to deliver, self-compacting capacity, safety, speed of construction, and environment-friendly, etc. Therefore, using

∗Corresponding author, Ph.D. Candidate, E-mail: hien_ise@yahoo.com
[a]Associated Professor, E-mail: sheen@kuas.edu.tw
[b]Associated Professor, E-mail: ljhuang@kuas.edu.tw

RMSM will reduce the labor cost and equipment cost compared to compacting conventional materials (Chen and Chang 2006, Lachemi *et al*. 2010). This material is neither concrete nor soil cement material, and may be named as soil-cement slurry or plastic soil-cement. Generally, RMSM mixture consists of quite small amount of Portland cement, fly ash or similar products, and a huge quantity of fine aggregate (soil), as well as tap water. Its 28-day unconfined compressive strength is 2 to 30 times greater than soil cement and can reach up to 5 MPa (Chen and Chang 2006). If future re-excavation is expected, the long-term compressive strength should be less than 1.4 MPa (Taha *et al*. 2007, Lachemi *et al*. 2010, Wu and Tsai 2009). This strength satisfies the demands of most compacted soil or granular fill. In recent years, spoil pile (e.g., native soil, reservoir, dreg silt) has been reported from literatures to be a feasible source for producing RMSM (Green 1999, Wu 2005, Wang and Tsai 2006, Finney *et al*. 2008, Wu and Lee 2011). In Taiwan, as a potential solution using on-site surplus earth, RMSM can be used as a backfill substituting for natural standard material (Chen and Chang 2006, Wu and Lin 2011, Sheen *et al*. 2012). The use of residual soil after excavation would provide a great benefit in reducing cost and consumption of natural recourses. Moreover, RMSM can be added several percentages of slag depending on specific task requirements. Slag in this paper refers to ground-granulated blast furnace slag, which is an industrial by-product obtaining from blast furnace in the production of cast iron. Slag is often used in concrete as supplementary cementitious material with a partial replacement to Portland cement to improve the workability and durability (Bouikni *et al*. 2009, Muhmood *et al*. 2009). The combined-cementitious application was well-known to provide an important key for both goals of economic and environmental protection.

In this study, an experimental plan was launched on RMSM using combination of river sand and on-site surplus soil as fine aggregate; slag was used as a cement substitution for partially replacing Portland cement with different levels (e.g., 0%, 10%, 20%, and 30%). Testing procedures were conducted on RMSM samples as per ASTM to evaluate its major engineering properties, viz. flowability, unconfined compressive strength, and ultrasonic pulse velocity (UPV). The findings from the experiment exhibit a potential solution of waste material consumption, which is necessary for sustainable development.

Predicting the compressive strength of RMSM from UPV is main aim of our work. To do this, two approaches were considered for analyzing. First, nonlinear regression method (RM) was used to build up the empirical UPV–strength relationship based on test data as usual. Second, artificial neural network (ANN) using combination of pulse velocity and other factors such as curing time, and mixed-composition as input of network was employed to interpolate the strength. Two kinds of back-propagation feed-forward neural network and one radial basis function neural network were applied to develop ANN models. Finally, the performance of two approaches (RM and ANN) in predicting was compared with the experimental results by measuring the statistical parameters.

2. Ultrasonic pulse velocity test

Among the available non-destructive test methods, ultrasonic pulse velocity technique is widely employed due to its advantages (Kawalramani and Gupta 2006, Trtnik *et al*. 2006, ASTM C597 2009). This approach based on measuring travel time over the previous known distance (known as velocity) in samples of compressive stress waves (P-waves). The ultrasonic pulse equipment consists of transmitter from which ultrasonic are transmitted, a receiver and timer. The quality, elastic properties of some materials are closely related to the pulse velocity (ASTM C597 2009). The compressive strength known as one of the most important characteristic in concrete is

conventionally evaluated from the empirical velocity–strength relationships often given by manufactures of device or built up by users.

3. Prediction models for compressive strength of RMSM

3.1 Artificial neural networks – FFNN and RBNN

Artificial neural networks, as the name implies, are simulating the functioning of human brain. The most important feature of biological brain is its ability to "*learn*" and "*adapt*" (Haykin 1999). In recent years, there have been many successful applications of artificial neural network in civil engineering. Some of them are aimed at predicting engineering properties of concrete material (Kawalramani and Gupta 2006, Trtnik *et al*. 2009, Alshihri and Azmy 2009, Sarıdemir 2009, Bilgehan and Turgut 2010), shear capacity of reinforced concrete deep beams (Arafa *et al*. 2011), strength capacity of concrete column (Öztekin 2012), behavior of thick plate structures on elastic foundation (Öztekin and Ozgan 2012), geotechnical engineering (Jaksa and Maier 2008, Gunaydin *et al*. 2010, Yilmaz and Kaynar 2011), and so on. Basic building block of neural network is neuron. Generally, a neuron is information processing system unit consisting of connecting link, summation with or without bias and activation function. Each neuron, as shown in Fig. 1, receives inputs and weights from neurons in previous layer. The weighted sum of inputs is used as argument for an activation function to form an output.

In mathematical terms, the output of a neuron is calculated by using Eqs. (1)-(2)

$$u = \sum_{j=1}^{m} w_j x_j + b \qquad (1)$$

$$y = f(u) \qquad (2)$$

where, $x_j (j = 1, 2, ..., m)$ is the input signal from previous layer; $w_j (j = 1, 2, ..., m)$ is the weight associated with x_j; m is the number of inputs; b is the bias; $f(\square)$ is the activation (or transfer) function, commonly used with the logsig and purelin forms (Shah *et al*. 2011)
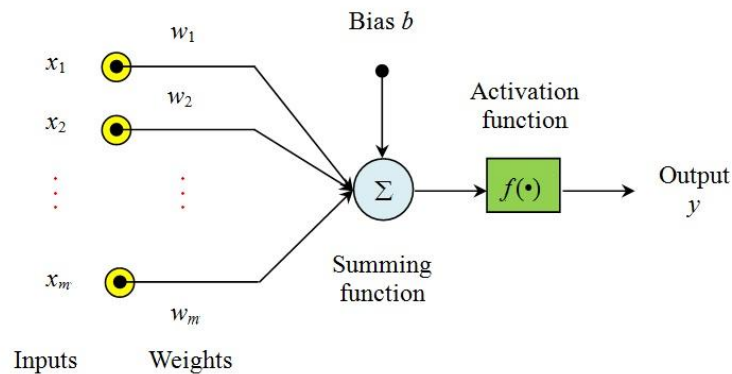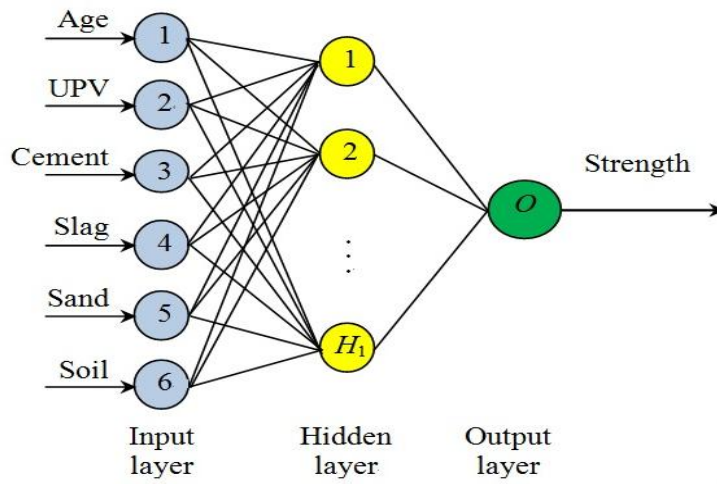

Fig. 1 Model of network block (Haykin 1999)

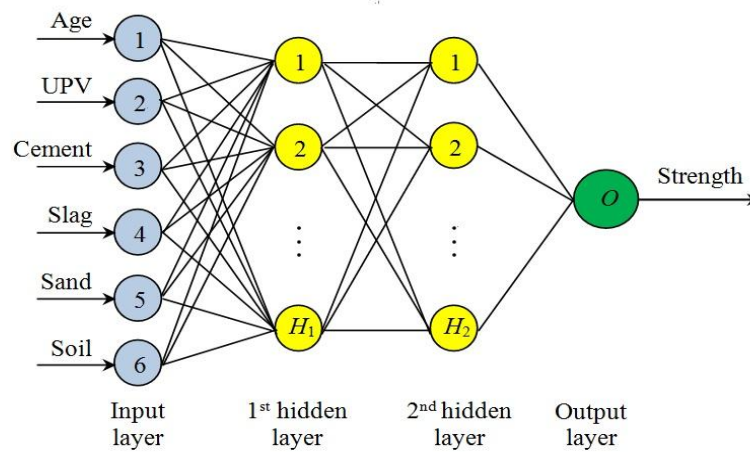Fig. 2 Structure of single hidden layer network used in the study

Fig. 3 Structure of single hidden layer network used in the study

Log-sigmoid transfer function (logsig)

$$f(u) = \frac{1}{1 + e^{-u}} \tag{3}$$

Linear transfer function (pureline)

$$f(u) = u \tag{4}$$

Usually, neurons in network are arranged in layer(s) as shown in Figs. 2-3. An ANN may be single or multi-layered. In a multi-layered network, layer(s) between input and output are called hidden layer(s). Existence of one or more hidden layers enables the network to extract a higher

complexity of approximate function (Haykin 1999). It is known that several types of neural networks have been developed to solve a specific problem. Multi-layered perceptron and Radial Basis function (RBF) neural networks were reported to be widely used for regression and classification (Yilmaz and Kaynar 2011, Wu and Wang 2012).

3.1.1 Feed-forward neural network (FFNN) with back-propagation training
In the case of multi-layered feed-forward neural network, outputs of each layer become inputs of next layer and there is no connection between neuron in the same layer. Back-propagation training is a process of calculation and adjustment the weights and biases so that the squared error between the output and target values of training set is minimized through number of iterations (epochs). The optimization technique is involved in using either the gradient or Jacobian of the network performance with respect to the weights (Sazli 2006, Beale *et al*. 2012). For the feed-forward network with back-propagation training, a number of learning algorithms have been effectively developed (e.g., Gradient Descent, Conjugate Gradient, Resilent back-propagation, Levenberg-Marquardt (L-M), etc). The L-M algorithm, belonged to nonlinear least square fitting method, is generally known to converge fast and more efficient for small and average size of ANNs (Beale *et al*. 2012).

3.1.2 Radial basis function neural network (RBNN)
An alternative kind of multi-layered feed-forward neural network is the radial basis function neuron network. Broomhead and Lowe (1988) were the first to exploit the use of RBF in the design of neural networks (Haykin 1999). Typically, RBNN comprises three layers, which are input, output and single hidden layer. In comparison with FFNN, RBNN have some advantages such as high training speed and less susceptible to problems with non-stationary inputs due to the behavior of the radial basis hidden units (Wu and Wang 2012). The major distinction between FFNN and RBNN is located at hidden neurons. FFNN often uses S-shaped sigmoid as activation function whereas RBNN widely uses Gaussian (bell-shaped) or other kernels. RBF has two parameters called centre and width (or spread), given in Eq. (6). The main characteristic of RBF is having its positive peak when Euclidean distance (norm) between input vector and center is zero and descends gradually as that norm increases. Furthermore, there are only weights connecting vector **w** between output and hidden layer. The outputs are formed by linear activation function, whose argument is weighted sum of all outputs generated from hidden neurons, as seen in Fig. 4.

For input vector $\mathbf{x}(x_1, x_2, ..., x_m)$, the kth output, $y_k(\mathbf{x})$, ($k = 1, 2, ..., M$) is given by Eqs. (5)-(6)

$$y_k(\mathbf{x}) = \sum_{j=1}^{H} w_{kj}\phi(\mathbf{x}, \mathbf{c}_j) + w_{k0} \tag{5}$$

$$\phi(\mathbf{x}, \mathbf{c}_j) = \mathrm{e}^{\left(-\frac{1}{2\sigma^2}\|\mathbf{x}-\mathbf{c}_j\|^2\right)} \tag{6}$$

where, w_{kj} and w_{k0} are the connecting weight from the jth hidden neuron and the bias to the kth output neuron, respectively; $\mathbf{c}_j(j=1,2,...,H)$ is the center of RBF at hidden neuron j^{th}; H and M are the number of hidden and output neurons, respectively; σ^2 is the spread of the Gaussian basis function, $\phi(\mathbf{x}, \mathbf{c}_j)$.

The training process of RBNN involves evaluating the parameters such as weights, centers, and
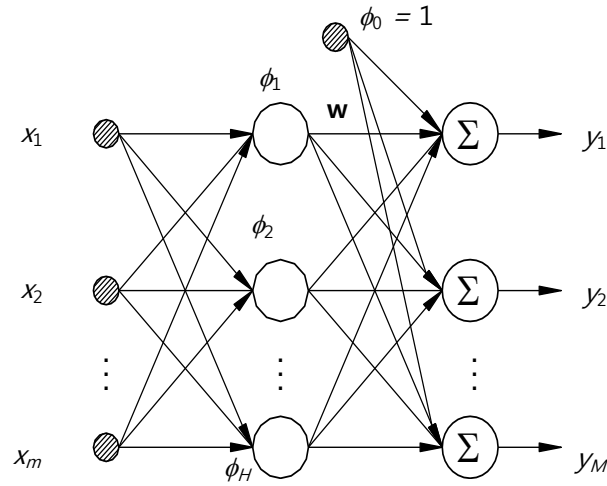
Fig. 4 A typical graph of radial basis neuron network

(a) Surplus soil   (b) River sand

Fig. 5 The soil and sand sample for experiment

widths. The centers can be either selected randomly from training set or determined by clustering or via learning procedure. In this investigation, centers were chosen as the second way. After determining the centers, the weights are adjusted based on minimize the square error between the output and target values of training set (Yilmaz and Kaynar 2011, Wu and Wang 2012).

3.2 Regression model

From test data results, a single-variable nonlinear expression for prediction of strength (R) from velocity (V) were derived by using regression method with a popular form as shown in the Eq. (7) (Trtnik *et al*. 2006)

$$R = a \cdot \mathrm{e}^{b \cdot V} \tag{7}$$

in which a and b are empirical parameters being widely known to vary for each proportion of constituents in mixtures; these coefficients will be evaluated from test results. However, due to complexities of materials, the ultrasonic waves propagate in structure are highly irregular. Therefore, in turn, accuracy of results is limited and using only pulse velocity for evaluating

strength may be inefficient (Kawalramani and Gupta 2006, Bilgehan and Turgut 2010). From this viewpoint, it is necessary to study the effect of material content in mixture on the relationship between pulse velocity and compressive strength. The proposed prediction models of the compressive strength will be discussed in the following sections.

4. Experimental program

4.1 Materials used and testing procedures

RMSM mixtures in this study contain Portland cement, slag, fine aggregate (the particle sizes range from 4.45 mm to 0.075 mm) and mixing with tap water. The fine constituent, which is usually an essential component, up to 80−85%, was created from three combinations of surplus soil and river sand with proportions of 6:4, 5:5, and 4:6. Primary soil was taken from construction site after basement excavation. It is a brown in color and clayey-sandy soil; the liquid limit (LL) and plastic index (PI) were found to be 22 and 2.3, respectively. In addition, this soil was classified as SP−SM in according with the USCS system (Das 2007). Meanwhile, the sand was obtained from the Laonung River in Taiwan with the fineness modulus (FM) of 2.57. The two primary material samples are illustrated in Figs. 5(a)-(b); and the physical properties were given in Table 1. Fig. 6 shows the grading curves of the sand and soil and its combinations used in the experiment. It is obviously seen that, only the sand meets the ASTM C33 (ASTM C33 2003) requirements of fine aggregate for making concrete. Next, Type I Portland cement conformed to the ASTM C150 (ASTM C150 2002) was employed; and slag, taken from China Steel Corporation, was partially replaced to cement as a cement substitution. A number of physical and chemical properties of the cement and slag for this work were shown in Table 2.

On the other hand, three groups of RMSM mixtures called M64, M55, and M46 corresponding with three combined ratios of sand: soil of 6:4, 5:5, and 4:6 were produced, respectively. In each group mix, the binder content (cement and slag) was fixed at 95 kg/m^3; the percentage of slag,.
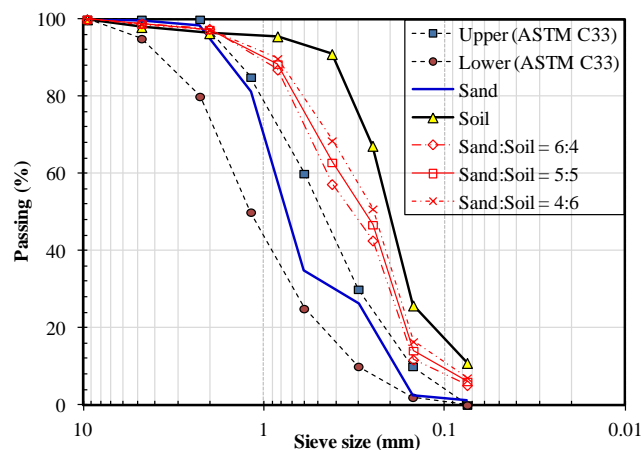

Fig. 6 The grading curve for sand, soil, and its combinations

Nain Y. Sheen, Jeng L. Huang and Hien D. Le

(a) Flowability test　　　　　　　　　　　(b) Ultrasonic pulse velocity test

Fig. 7 The grading curve for sand, soil, and its combinations

Table 1 Physical properties of river sand and surplus soil

Fine aggregates	Value
River sand:	
- Gravity (g/cm^3)	2.66
- Water absorption (%)	3.50
- Fineness modulus (FM)	2.57
Surplus soil (from basement excavation):	
- Gravity (g/cm^3)	2.69
- Optimum Moisture content (%)	12.0
- Liquid limit (LL)	22.0
- Plastic limit (PL)	19.7
- Plastic index (PI)	2.30
- Fineness modulus (FM)	1.24

Table 2 Chemical and physical properties of cement and slag

Properties	Portland cement, Type I (Taiwan cement corp.)	Slag (China steel corp.)
Chemical analysis (%)		
Silicon dioxide, SiO_2	20.87	33.82
Aluminum oxide, Al_2O_3	4.56	14.11
Ferric oxide, Fe_2O_3	3.44	0.34
Calcium oxide, CaO	63.14	41.04
Magnesium oxide, MgO	2.82	6.96
Sulfur trioxide, SO_3	2.06	0.70
Loss of ignition, LOI	2.30	0.35
Physical properties		
Fineness, Blaine (cm^2/g)	3851	4390
Specific gravity	3.15	2.89

which was in replacement of cement, varied from 0%, 10%, 20%, to 30%; water-to-binder ratio (*w/b*) and water-to-solid ratio (*w/s*) was selected at 3.4 and 0.2, respectively after few trials. Table 3 presents the mix-proportions of RMSM using in the study.

Flowability test for fresh RMSM mixtures was conducted according to ASTM D6103 (ASTM D6103 1997). The flow slump was measured with an opened-end cylinder of 75 × 150 mm, as

shown in Fig. 7(a). Design goal for spread tube slump ranges from 150 mm to 300 mm in accordance with many applications. As regards compression test, after casting cylinders of 150 mm by 300 mm, the specimens were covered with plastic sheets for 48 hours prior demoulding. The cylinders were carefully stored in laboratory room for curing under environmental condition of 100 % relative humidity and 23°C. When reaching the curing ages of 1-, 7-, 28-, 56-, and 91 days, the ultrasonic pulse velocity test was carried on the cylinders as per ASTM C597 (ASTM C597 2009), as seen in Fig. 7(b). Compressive strength test conformed to ASTM D4832 (ASTM D4832 2002) was done thereafter by applying an axial force on these cylindrical specimens to failure.

4.2 Testing results

The test data results for cylindrical tube flow of fresh RMSM were shown in Table 3. It is observed that all of samples were well achieved the flowability requirement of 150-300 mm. In addition, with the water-to-binder ratio being fixed, there is a tendency of improving the flow consistency as the percentage of slag replacement increases.

Table 4 illustrates the results of unconfined compressive strength and associated pulse velocity at different curing ages. The 28-day strength was ranged from 0.41 to 0.84 MPa while the 91-day strength was slightly higher, varied from 0.45 to 0.90 MPa; and it completely meets the strength requirement of re-excavation because of being less than 1.4 MPa (Lachemi *et al.* 2010).

Fig. 8(a) displays the strength development of RMSM with group samples of M64, M55, and M46. It is evident that strength ratio $R(t)/R(28)$ (comparing to the 28-day strength) was improved for long-term period due to hydration of cement and slag. Also, the 91-day strength was observed to be approximately 10% higher than that of 28 days. This finding is quite consistent with the study published in literature (Chen and Chang 2006).

In addition, Fig. 8(b) demonstrates the influence of slag replacement level to the compressive strength for group M64, M55, as well as M46. It indicates that when the Portland cement was replaced by slag, the compressive strength had a significant reduction compared to the control mix

Table 3 Mix-proportions, density, and tube flow of RMSM

| Group No.	Sand: soil ratio[b]	Cement (kg/m³)	Slag (kg/m³)	Sand (kg/m³)	Density (kg/m³)	Tube flow (mm)
M64-0[a] (control)		95	0	1000	2093	156
M64-10[a]	6:4	85.5	9.5	1000	2092	164
M64-20[a]		76	19	1000	2091	205
M64-30[a]		66.5	28.5	999	2091	223
M55-0[a] (control)		95	0	834	2095	161
M55-10[a]	5:5	85.5	9.5	833	2094	200
M55-20[a]		76	19	833	2093	220
M55-30[a]		66.5	28.5	833	2093	245
M46-0[a] (control)		95	0	667	2097	187
M46-10[a]	4:6	85.5	9.5	667	2096	221
M46-20[a]		76	19	666	2095	257
M46-30[a]		66.5	28.5	666	2095	270

[a]percentage of slag replacement to cement; [b] proportion of sand to soil in mixtures
Binder, included cement and slag, was fixed at 95 kg/m³; water-to-binder ratio (*w/b*) = 3.4

Table 4 Ultrasonic pulse velocity V (m/s) and compressive strength R (MPa) at various ages

Group No.	Ages (days)									
	01		07		28		56		91	
	V	R	V	R	V	R	V	R	V	R
M64-0	590	0.226	917	0.579	1044	*0.845**	1070	0.883	1090	0.903
M64-10	550	0.187	830	0.493	967	**0.768**	982	**0.806**	1005	0.823
M64-20	470	*0.169**	800	0.447	940	0.659	950	0.687	960	0.716
M64-30	540	0.151	860	0.393	986	0.590	995	**0.610**	1032	*0.649**
M55-0	490	*0.215**	790	0.494	930	0.732	947	0.772	957	**0.801**
M55-10	430	*0.177**	750	*0.440**	877	0.671	899	0.718	905	0.754
M55-20	520	0.159	796	**0.413**	917	0.640	943	0.667	963	**0.678**
M55-30	440	**0.147**	753	0.366	897	0.585	917	0.616	927	0.627
M46-0	400	0.188	720	0.458	845	0.611	870	*0.621**	880	*0.641**
M46-10	490	0.160	767	0.413	888	0.533	901	0.548	926	0.578
M46-20	390	0.152	722	0.377	861	0.471	878	*0.493**	890	0.524
M46-30	327	0.140	692	**0.337**	818	0.413	842	0.423	855	**0.446**

Note: The series of 9 data points in testing set is marked with asterisks (*); the series of 9 data points in alidation set is marked with bold numbers.
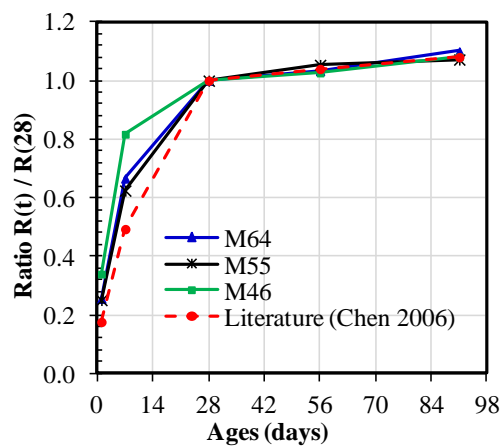
(a) Strength development with time (comparing to the 28-day strength)
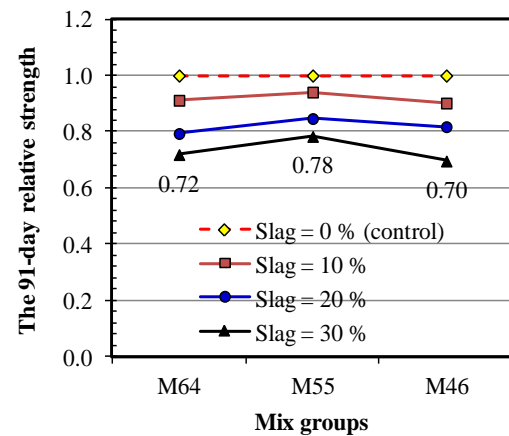
(b) The 91-day relative compressive strength (comparing to the control)

Fig. 8 Strength development and the effect of slag replacement ratio

(without slag) due to slow pozzolanic reaction of slag. For instance, at slag substitution level of 30%, the 91-day strength was found to achieve about 72%, 78%, and 70% of the control for group M64, M55, and M46, respectively. This behavior is expected and known in advance because slag has been reported to be low in the CaO/SiO_2 ratio and not as good as Portland cement in contribution of strength development. Moreover, test data in Table 4 points out that rising up the soil constituent in mixture would contribute to a remarkable strength fall. For example, as the sand−soil proportion varies from 6:4 to 4:6, the strength had a dramatic drop of 31% comparing to the control on averages.

5. Data analyses

5.1 Proposed neural networks

In this paper, the FFNN with one and two hidden layers (namely ANN-I, ANN-II, respectively) and RBNN (ANN-III) were developed for predicting the strength, as shown in Figs. 2-3. Three of these ANN topologies have the same input and output layer; the difference is in the hidden layer. The input layer has six neurons, which denote the UPV, age and proportions in mix design (cement, slag, sand, and soil); the output layer has only one neuron representing predicted strength development at the ages from one to 91 days of curing. Mathematically, the input−output mapping can be generally expressed as Eq. (8)

$$R = F \text{ (age, UPV, cement, slag, sand, soil)} \tag{8}$$

There were 60 experimental data points (input−output pairs) in total, as shown in Table 4. In the case of ANN implementation (FFNN and RBNN), the data set (N_{all} = 60) was first scaled in range of [-1; 1] for accelerating training speed. Next, it was randomly divided into three subsets such as training set (70% of total, corresponding to N_{train} = 42 data points), testing set (15% of total, corresponding to N_{test} = 9 data points), and validation set (15% of total, N_{val} = 9 data points), as seen in Table 4. The errors derived from validation set were monitored during training process for preventing the over-training phenomenon.

The sigmoid function (logsig) was used as activation in hidden layer(s), whereas linear function (pureline) was used for output layer when FFNN was implemented. In this work, neural network Toolbox in Matlab (2010) was employed for analysis. In configuration of ANNs, it is important to determine logically the number of hidden neurons and there is no general rule (Trtnik *et al*. 2006, Alshihri and Azmy 2009). This number must be low enough to ensure generalization. Too many hidden neurons would lead to over-fitting. Previous researchers have proposed some experiences to select the number of neurons in hidden layers (i.e., upper bound for required number of hidden neurons should be one greater than twice the number of input units; the ratio of 3:1 between number of neurons in first and second hidden layer (Alshihri and Azmy 2009)). However, these rules do not guarantee the optimal solution for all ANNs. Consequently, the number of neurons in hidden layer should be decided after few trials.

To examine the performance of each model, which one is better closed to the experimental results, following three indices were employed to evaluate as Eqs. (9-11) (Samarasinghe 2007, Bilgehan 2010)

Root mean square error (*RMSE*)

$$RMSE = \sqrt{\frac{1}{N} \sum_{i=1}^{N} \left(t_i - z_i \right)^2} \tag{9}$$

Mean absolute percentage error (*MAPE*)

$$MAPE(\%) = \frac{1}{N} \sum_{i=1}^{N} \left| \frac{t_i - z_i}{z_i} \right| \cdot 100 \tag{10}$$

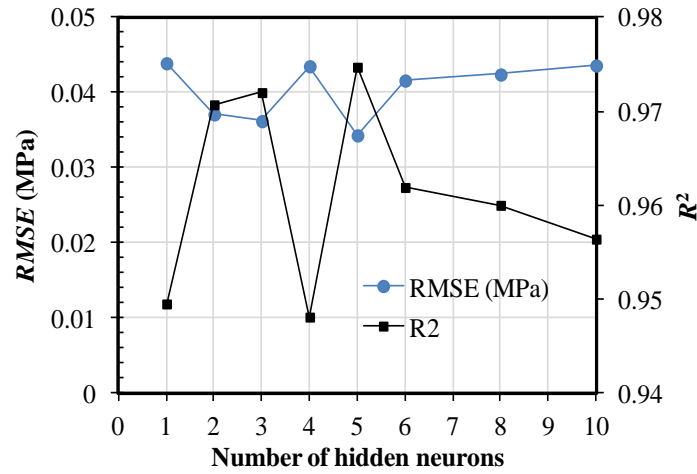Fig. 9 Performance of ANN-I with difference number of hidden neurons

Table 5 The information of ANN parameters

No.	Network parameters	FFNN		RBNN
		ANN-I	ANN-II	ANN-III
1.	Number of input neurons	6	6	6
2.	Number of output neurons	1	1	1
3.	Number of 1st hidden neurons	5	3	27
4.	Number of 2nd hidden neurons	-	2	-
5.	Activation function used: + Hidden layer + Output layer	Sigmoid Pureline	Sigmoid Pureline	Gaussian Linear
6.	Training algorithm	L-M (trainlm)	L-M (trainlm)	Radial basis (newrb)
7.	Mean square error (mse)	0.0013	0.0007	0.001
8.	Epochs	7	13	22

The coefficient of determination (R^2)

$$R^2 = 1 - \frac{\sum_{i=1}^{N}(t_i - z_i)^2}{\sum_{i=1}^{N}(t_i - \bar{t})^2} \tag{11}$$

here t_i and z_i denote actual (or target) and predicting (or output) value, respectively; $\bar{t}$ is the average value of target; N is the number of data points.

It is noticed that, the value of R^2 is near 1.0, and the value of *MAPE, RMSE* are as small as zero, there will be a better prediction and vice versa. For ANN-I, as shown in Fig. 2, the number of hidden neurons were varied from low to high. With specific number of hidden neurons, the network was trained with several times and its performance was evaluated through averaging of

statistic parameters (*RMSE* and R^2). Fig. 9 displays the variation of *RMSE* and R^2 versus different hidden neuron numbers. It is indicated that single hidden layer with five neurons is the reasonable solution for ANN-I due to optimal value of *RMSE* (min) and R^2 (max). With ANN-II, fixed with five hidden neurons, scheme being two hidden layers of three and two neurons was proposed to analyze, as illustrated in Fig. 3. For ANN-III, the number of hidden neurons was determined during training process. The procedure was repeatedly done by adding to network one hidden neuron at a time until the mean square error falls beneath an error goal or maximum number neuron has been achieved (Beale *et al*. 2012). The goal error for training ANN-III was set approximation to the mean square error value in the ANN-I and ANN-II. Summary of parameters of the trained-ANNs were tabulated in Table 5.

5.2 Regression model (RM)

For strength evaluation, the empirical *R-V* correlation had been built up by means of single regression analysis. Least square error for curve fitting was employed to generate the equation of correlation. The test results (51 data points), excluding testing set (9 data points), as shown in Table 4, were employed to generate the exponential formula as Eq. (12). And Fig. 10 shows the graph of interpolated curve and all data points from the experiment.

$$R = 0.0477 \cdot e^{0.0028V}$$

(12)

From the expression and experimental data, we know it is a nonlinear relationship.

Table 6 Statistic parameters for RM, ANN-I, ANN-II and ANN-III model

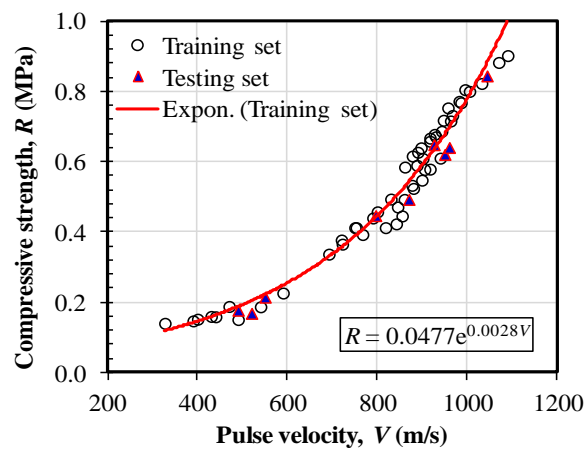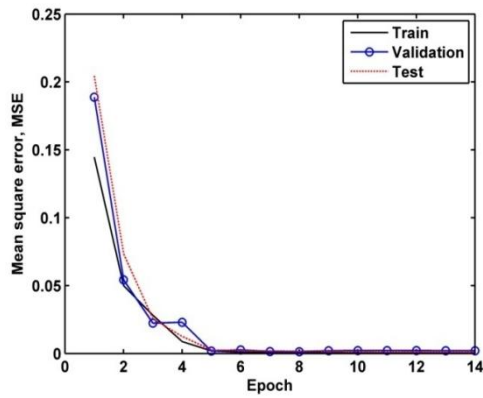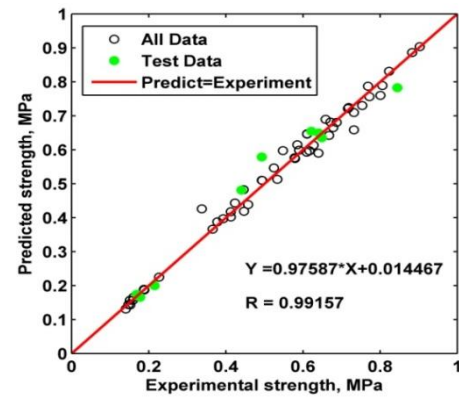| Model	Training data			Testing data		
	RMSE (MPa)	*MAPE* (%)	R^2	*RMSE* (MPa)	*MAPE* (%)	R^2
RM	0.0466	7.0387	0.9526	0.0387	6.8262	0.9712
ANN-I	**0.0224**	**3.1612**	**0.9889**	**0.0404**	**6.4309**	**0.9687**
ANN-II	0.0265	4.2038	0.9844	0.0419	7.1190	0.9661
ANN-III	0.0344	5.8523	0.9741	0.0460	7.9515	0.9593

Fig. 10 The pulse velocity–strength relationship
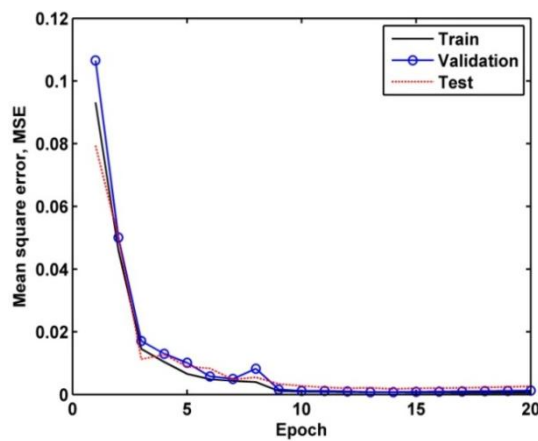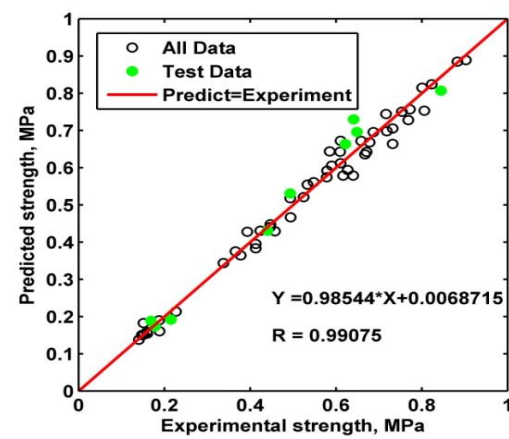
(a) Mean square error

(b) Cross-correlation of predicted and actual strength

Fig. 11 The performance of ANN-I

(a) Mean square error

(b) Cross-correlation of predicted and actual strength
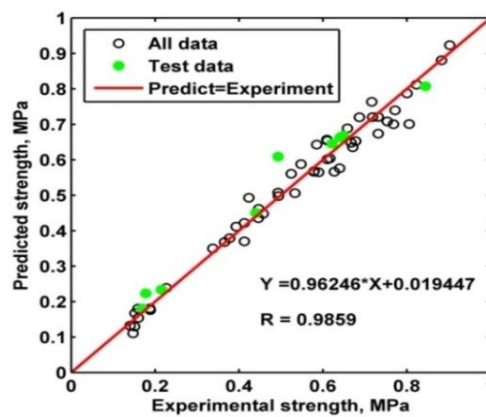
Fig. 12 The performance of ANN-II

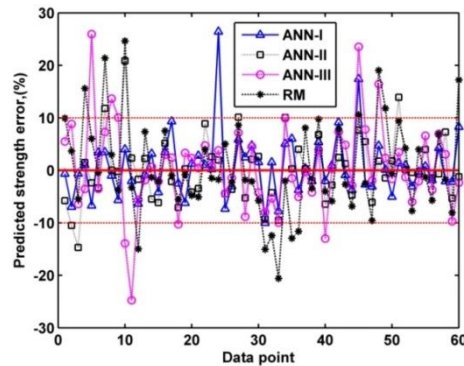Fig. 13 Cross-correlation of predicted and actual strength for ANN-III

Fig. 14 The predicted strength error for different models

6. Results and discussions

The development of compressive strength, which was predicted by ANNs at the different ages, were shown in Figs. 11-13 in comparison with the measured strength. Fig. 11(a) and 12(a) display the performance (mean square error) of ANN-I and ANN-II, respectively. And, no overtraining was observed for both the models. Figs. 11(b), 12(b), and 13 graphically illustrate the cross-correlation of the predicted and observed strength and all show good predicted results. This is evidenced by the fact that the points (their coordinates are measured and predicted strength) were located very close to the bisector passing through the origin (the solid line). The degree of correlation between predicted versus actual values was estimated by R^2, *RMSE*, and *MAPE*; and these parameters were presented in Table 6.

Accordingly, it is believed that all the schemes are well reasonable for strength prediction due to excellence in the error estimation parameters for both of training and testing set. Therefore, the proposed ANN models have a well-evaluated capacity. As seen in Table 6, for the ANN-I, the values of *RMSE*, *MAPE* were 0.0404 MPa, and 6.4309%, respectively, and these parameters were found to be slightly lower than those of ANN-II, ANN-III for testing data. In addition, the coefficient of determination (R^2) was observed to be highest for RM (0.9712) and the followings were ANN-I (0.9687), ANN-II (0.9661), and ANN-III (0.9593). Meanwhile, as regards the R^2, the aforementioned sequence was ANN-I, ANN-II, ANN-III, and RM for training data. Consequently, among the three ANN frameworks, the ANN-I would be the best model in predicting the compressive strength. Also, the outcome of ANN-I could be comparable with the RM when the testing data was examined, and it is significantly better in accuracy when the training data was investigated due to being higher in R^2 (0.9889 compared to 0.9526). In summary, it implies that ANN-I model is greatly acceptable for determining the strength of RMSM specimens.

Moreover, to evaluate the efficiency and precision of these prediction models, predicted strength errors defined as percentage error between the predicted and experimental strength of all models were plotted in Fig. 14. It can be seen that, almost the predicted strength interpolated from ANN approach is well approximate to the actual values for error estimation within ± 10 %, and there are few values fallen out of this range. In particular, the ANN-I has only two undesirable points, whereas model RM has 14/60 unexpected points because the performance of RM is not as good as of ANNs for training data.

7. Conclusions

In order to evaluate the compressive strength development of RMSM at the different ages, e.g., 1-, 7-, 28-, 56-, and 91 days, an experimental program was conducted for the study. The conventional method of UPV and compressive test on the same cylinders of 150 mm by 300 mm were employed for investigation. Then we considered two approaches for prediction of compressive strength from UPV and/or other parameters: RM and ANN. In RM, an empirical exponential UPV–compressive strength correlation for RMSM based on testing results was built-up and represented. On the other hand, artificial neural networks with three schemes were successfully proposed for prediction, namely ANN-I, ANN-II and ANN-III. In the neural network models, the first two are FFNN and the last is RBNN. In ANN-I, single hidden layer with five neurons was chosen based on number of hidden neuron parametric study, whereas ANN-II with the same hidden neuron as ANN-I, but divided in to two hidden layers of three and two neurons for the first and second hidden layer, respectively. Radial basis neural network was applied to develop the ANN-III. Results generated from the three ANN topologies are proved to be highly accurate. The strength from RM and ANN prediction were made a comparison with each other by measuring the error estimation parameters such as *RMSE, MAPE*, and R^2 as well. As a result, the compression strength predicted from the well-trained ANN models is closer to the actual than RM model interpolated from UPV only. In addition, results on this investigation show that among the three of ANN topologies, ANN-I give the best performance for interpolation because it has the lowest *RMSE* and *MAPE* and the highest R^2 simultaneously. In fact, almost the strength provided from ANN-I have the errors, which do not exceed 10 % comparing to the actual values.

Acknowledgements

References

ACI Committee 229 (2005), *Controlled Low-Strength Materials*, American Concrete Institute, Farmington Hills, MI, USA.

Alshihri, M.M. and Azmy, A.M. (2009), "Neural networks for predicting compressive strength of structural light weight concrete", *J. Construct. Build Mater.*, **23**, 2214-2219.

Arafa, M., Alqedra, M. and An-Najjar, H. (2011), "Neural network model for predicting shear strength of reinforced normal and high-strength concrete deep beams", *J. Appl. Sci.*, **11**(2), 266-274.

ASTM C150 (2002), *Standard specification for Portland cement*.

ASTM C33 (2003), *Standard specification for concrete aggregates*.

ASTM C597 (2009), *Standard test method for pulse velocity through concrete*.

ASTM D4832 (2002), *Standard test method for preparation and testing of controlled low strength material (CLSM) test cylinders*.

ASTM D6103 (1997), *Standard test method for flow consistency of controlled low strength material*.

Beale, M.H., Hagan, M.T. and Demuth, H.B. (2012), *Neural network toolbox user's guide*, Mathworks.

Bilgehan, M. and Turgut, P. (2010), "The use of neural networks in concrete compressive strength estimation", *J. Comput. Concr.*, **7**(3), 271-283.

Bouikni, A., Swamy, R.N. and Bali, A. (2009), "Durability properties of concrete containing 50% and 65%

slag", *J. Construct. Build Mater.*, **23**, 2836-2845.

Chen, J.W. and Chang, C.F. (2006), "Development and application of the ready-mixed soil material", *J. Mater. Civil Eng.*, **18**(6), 792-799.

Das, B.M. (2007), *Principles of Geotechnical Engineering*, (7th Edition), Cengage Learning.

Finney, A.J., Shorey, E.F. and Anderson, J. (2008), "Use of native soil in place of aggregate in controlled low strength material (CLSM)", *International Pipelines Conference 2008*, Atlanta, United States, 1-13.

Green, B.H. (1999), *Development of soil-based controlled low-strength materials*. Technical report INP-SL-2, prepared for U.S. Army Corps of Engineers.

Gunaydin, O., Gokoglu, A. and Fener, M. (2010), "Prediction of artificial soil's unconfined compression strength test using statistical analyses and artificial neural networks", *J. Adv. Eng. Softw.*, (**41**), 1115-1123.

Haykin, S. (1999), *Neural networks, a comprehensive foundation*, (2nd Edition), Prentice Hall.

Jaksa, M.B. and Maier, H.R. (2008), "Future challenges for artificial neural network modeling in geotechnical engineering", *The 12th International Conference of International Association for Computer Methods and Advances in Geomechanics (IACMAG)*, India.

Kawalramani, M.A. and Gupta, R. (2006), "Concrete compressive strength prediction using ultrasonic pulse velocity through artificial neuron networks", *J. Automat. Construct.*, **15**, 374-379.

Lachemi, M., Sahmaran, M., Hossain, K.M.A., Lotfy, A. and Shehata, M. (2010), "Properties of controlled low-strength materials incorporating cement kiln dust and slag", *J. Cement Concrete Compos.*, **32**(8), 623-629.

Muhmood, L., Vitta, S. and Venkateswaran, D. (2009), "Cementitious and pozzolanic behavior of electric arc furnace steel slags", *J. Cement Concrete Res.*, **39**, 102-109.

Ö ztekin, E. and Ozgan, K. (2012), "Analysis of thick plates on elastic foundation by back-propagation artificial neural network using one parameter foundation model", *J. Eng. Appl. Sci.*, **4**(1), 66-76.

Ö ztekin, E. (2012), "Prediction of confined compressive strength of square concrete columns by artificial neural networks", *J. Eng. Appl. Sci.*, **4**(3), 17-35.

Samarasinghe, S. (2007), *Neural Networks for Applied Sciences and Engineering*, Auerbach Publications.

Sarıdemir, M. (2009), "Prediction of compressive strength of concretes containing meta-kaolin and silica fume by artificial neural networks", *J. Adv. Eng. Softw.*, **40**, 350-355.

Sazli, M.H. (2006), "A brief review of feed-forward neural network", *Commun. Fac. Sci. Univ. Ank*, *Series A2-A3*, **50**(1), 11-17.

Shah, A.A., Alsayed, S.H., Abbas, H.Y. and Al-Salloum, A. (2012), "Predicting residual strength of non-linear ultrasonically evaluated damaged concrete using artificial neural network", *J. Construct. Build. Mater.*, **29**, 42-50.

Sheen, Y.N., Huang, L.J., Le, D.H. and Zhang, L.H. (2012), "Application of artificial neural networks in predicting concrete compressive strength from pulse velocity tests", *The Eleventh National Conference on Structural Engineering*, Taiwan, September.

Taha, R.A., Alnuaimi, A.S., Al-Jabri, K.S. and Al-Harthy, A.S. (2007), "Evaluation of controlled low strength materials containing industrial by-products", *J. Build Environ.*, **42**, 3366-3372.

Trtnik, G., Kavčič, F. and Turk, G. (2009), "Prediction of concrete strength using ultrasonic pulse velocity and artificial neural networks", *J. Ultrasonic*, **49**, 53-60.

Wang, H.Y. and Tsai, K.C. (2006), "Engineering properties of lightweight aggregate concrete made from dredged silt", *J. Cement Concrete Compos.*, **28**, 481-485.

Wu, J.Y. (2005), "Soil-based flowable fill for pipeline construction", *ASCE, Proceedings of Pipelines 2005: Optimizing Pipeline Design, Operations, and Maintenance in Today's Economy*, Houston, Texas, USA.

Wu, J.Y. and Lee, M.Z. (2011), "Beneficial reuse of construction surplus clay in CLSM", *Int. J. Pavement Res. Technol.*, **4**(5), 293-300.

Wu, J.Y. and Lin, Y.J. (2011), "Experimental study of reservoir siltation as CLSM for backfill applications", *Proceeding of Geo-Frontiers*, Texas, March, 1217-1226.

Wu, J.Y. and Tsai, M. (2009), "Feasibility study of a soil-based rubberized CLSM", *J. Waste Manag.*, **29**, 636-642.

Wu, Y. and Wang, H. (2012), *Using Radial Basis Function Networks for Function Approximation and Classification*, International Scholarly Research Network, ISRN Applied Mathematics, Article ID 324194, 34 pages.

Yilmaz, I. and Kaynar, O. (2011), "Multi regression ANN (RBF, MLP) and ANFIS models for prediction of swell potential of clayey soils", *J. Exp. Syst. Appl.*, **38**, 5958-5966.

CC